ACS OMEGA

http://pubs.acs.org/journal/acsodf

Article

Synthesis and Self-assembly of Novel Nanofeather-like Fluorescent Alkyloxy-Containing Diphenyl Ether Organogelators

Matokah M. Abualnaja, Abdulmajeed F. Alrefaei, Hana M. Abumelha, Omaymah Alaysuy, Amal T. Mogharbel, Albandary Almahri, and Nashwa M. El-Metwaly*

Cite This: *ACS Omega* 2022, 7, 34309−34316

Read Online

ACCESS | Metrics & More | Article Recommendations | Supporting Information

ABSTRACT: In this study, novel fluorescent low molecular-weight organogelators are derived from diphenyl ethers and substituted with para-alkoxy groups of different aliphatic chain lengths. The present research promotes the preparation of innovative nanofeather-like assemblies from the synthesized diphenyl ether-derived organogelators. The gelation performance of the prepared alkoxy-substituted diphenyl ethers was reported. The synthesis procedure was achieved by using a base-catalyzed reaction of hydroxyl-substituted diphenyl with various alcohols of different aliphatic chain lengths. The chemical structures of the synthesized diphenyl ether derivatives were studied by $^{1}H/^{13}C$ NMR and infrared spectroscopy. Fluorescence and UV−vis absorption spectral analyses showed solvatochromism. The diphenyl ether derivatives with longer alkoxy terminal substituents showed enhanced thermoreversible gelation activity as compared to the diphenyl ether derivatives with shorter alkoxy terminal substituents. The morphological properties of the self-assembled diphenyl ethers were studied by transmission electron microscopy and scanning electron microscopy, which showed supramolecular architectures of highly ordered nanofeathers, enforced by van der Waals interactions and π-stacks. Depending on the length of the aliphatic tail, different morphologies were detected, including nanofeathers, nanofibers, and nanosheets. The antimicrobial and cytotoxic properties of the prepared diphenyl ether-derived organogelators were examined to confirm their possible use in various fields like drug delivery systems.

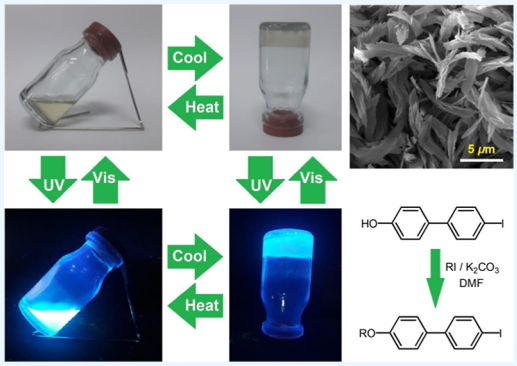

1. INTRODUCTION

Low molecular-weight organogelators are becoming more relevant owing to their thermal reversibility, sensitivity to chemicals, and diversity of macroscaled architectures. Biomedical, foodstuff, and cosmetic applications have all exploited organogel technology.[1−4] The self-assembly of small organogelator molecules occurs by the entrapment of tolerable volumes of solvents, providing beneficial characteristics for various applications. Self-assembled structures can introduce optoelectronic characteristics like enhancing emission and charge transfer.[5−16] A supramolecular organogel can be described as a soft matter consisting of a viscoelastic non-flowing fluid due to the existence of an organogelator capable of self-assembling into three-dimensional supramolecular architectures. Those supramolecular architectures can be generated in a variety of morphologies, such as nanofeathers, nanoribbons, nanosheets, nanorods, and nanofibers.[17,18] Self-assembly of organogelators has interesting research in many fields, such as catalysis, sensors, pollutant removal, drug self-delivery, and tissue engineering. The self-assembly processes are usually driven by various types of attraction forces such as physical bonding, chemical bond formation, phase transition, and/or cross-linking.[19−21] Recently, the distinctive capability of organic gelators to uphold solvents by non-covalent bond formation, like H-bonds, π-stacks, and van der Waals forces, has received considerable attention.[22−25] The organoelator molecular entities typically self-assemble into highly ordered macro-molecular architectures without exchanging into their dense structural form. Low molecular-weight organogels have been used in the formation of nanoporous substrates, removal of pollutants, enhancement of rheological properties in cosmetic products, drug delivery, sensors, engineering of tissues, foodstuffs, and polymer crystalline nucleation substances.[26−31]

Iodo-substituted compounds have been reported as efficient organic gelators, while their corresponding hydrogen-substituted derivatives are not. Recently, iodine substitution was found to highly improve the gelation properties of various materials.[32,33] Despite their importance in many applications,

Received: June 20, 2022
Accepted: September 8, 2022
Published: September 16, 2022

https://doi.org/10.1021/acsomega.2c03838
ACS Omega 2022, 7, 34309−34316

the development of luminous organogelators based on alkoxy-substituted diphenyl ethers has been described in limited studies.[34,35] Moreover, the development of fluorescent nano-feather-like organic gelators based on alkoxy-substituted diphenyl ethers has not been reported yet. In the current study, organogelators with novel fluorescent alkoxy-substituted diphenyl ethers have been synthesized, characterized, and self-assembled for potential optoelectronic applications. Organogels made of diphenyl ether hard cores and flexible terminal alkoxy chains have been described. The synthesis procedure was achieved by a base-catalyzed reaction of hydroxyl-substituted diphenyl with various alcohols of different aliphatic chain lengths. As a result, diphenyl ethers with high emission and extended conjugation were produced. The emission of these alkoxy-substituted diphenyl ethers with various alkoxy chain lengths was reported. As a consequence, they could be considered proper materials for optoelectronic display devices with reduced energy usage, in particular, portable displays.[36,37] Alkoxy-substituted diphenyl ether derivatives were tested for gelation and supramolecular characteristics in different solvents. The critical gel concentration (CGC) of a formed gel was recorded in various solvents. Alkoxy-substituted diphenyl ethers were tested for antibacterial efficacy and cytotoxicity. Both scanning electron microscopy (SEM) and transmission electron microscopy (TEM) were utilized to examine the nanostructured morphologies of self-assembled fluorescent organogels. The prepared diphenyl ethers displayed solvatochromic and solvatofluorochromic properties.

2. EXPERIMENTAL SECTION

2.1. Materials and Reagents. The materials utilized in the current research were sourced from commercial sources. *n*-Iodoalkane, 4-(4-iodophenyl)phenol, potash, and *N*,*N*-dimethylmethanamide were purchased from Merck and Sigma-Aldrich (Egypt). All solvents were of spectroscopic grade and obtained from Fluka and Sigma-Aldrich (Egypt). The organogelators were synthesized according to previous procedures.[38] Under ultraviolet light, aluminum plates coated with a thin layer of silica gel (60) were used to monitor the reaction progress by thin layer chromatography (TLC) (UV_{254}). Flash column chromatography was used to purify the produced chemicals using silica gel 60. Both fibroblast cell lines and bacteria, including *Staphylococcus aureus* (ATCC 29213) and *Escherichia coli* (ATCC 25922), were obtained from the American Type Culture Collection (ATCC, Rockville, MD, USA).

2.2. Synthesis Procedures. *2.2.1. General Synthesis of 4-Alkoxy-4′-iodobiphenyl.* *n*-Iodoalkane, 4-(4-iodophenyl)-phenol, and potash were dissolved in *N*,*N*-dimethylmethanamide in a nitrogen atmosphere. The provided solution was stirred for 9 h till TLC indicated a complete consumption of 4-(4-iodophenyl)phenol. The reaction mixture was then poured into crushed ice. The generated precipitate was filtered, washed with distilled water, and air-dried.

2.2.2. 4-Propyloxy-4′-iodobiphenyl **1**. 4-Propyloxy-4-iodobiphenyl **1** was synthesized from an admixture of 4-(4-iodophenyl)phenol (1.52 g; 5 mmol), *n*-iodopropane (1.72 g, 8.5 mmol), dimethylformamide (DMF) (10 mL), and potash (1.40 g; 10 mmol) and re-crystallized from ethyl alcohol (100%) to afford white crystals (3.0 g; 90%); ^{1}H NMR (400 MHz, $CDCl_3$): 7.77 (d, 2H), 7.51 (d, 2H), 7.34 (d, 2H), 6.91 (d, 2H), 4.00 (t, 2H), 1.88 (m, 2H), 1.08 (t, 3H); IR (ν/cm^{-1}): 3046, 2964, 2934, 2877, 1730; Elemental Analysis ($C_{15}H_{15}IO$: 338.18) Calcd: C, 53.27; H, 4.47. Found: C, 53.04; H, 4.38.

2.2.3. 4-Hexyloxy-4′-iodobiphenyl **2**. It was synthesized from a mixture of 4-(4-iodophenyl)phenol (1.73 g; 5 mmol), *n*-iodohexane (1.75 g; 8.5 mmol), DMF (10 mL), and potash (1.40 g; 10 mmol) and re-crystallized from absolute ethanol to give a white powder (1.71 g; 91%); ^{1}H NMR (400 MHz, $CDCl_3$): 7.78 (d, 2H), 7.51 (d, 2H), 7.32 (d, 2H), 7.00 (d, 2H), 4.03 (t, 2H) 1.85 (m, 2H), 1.52 (m, 2H), 1.41 (m, 4H), 0.97 (t, 3H); IR (ν/cm^{-1}): 2953, 2861; Elemental Analysis ($C_{18}H_{21}IO$: 380.26) Calcd: C, 56.85; H, 5.57. Found: C, 56.77; H, 5.42.

2.2.4. 4-Undecyloxy-4′-iodobiphenyl **3**. It was synthesized from an admixture of 4-(4-iodophenyl)phenol (1.98 g; 5 mmol), *n*-iodoundecane (1.75 g; 6 mmol), DMF (10 mL), and potash (1.40 g; 10 mmol) and re-crystallized from absolute ethanol to give a white powder (2.21 g; 95%); ^{1}H NMR (400 MHz, $CDCl_3$): 7.76 (d, 2H), 7.50 (d, 2H), 7.34 (d, 2H), 6.98 (d, 2H), 4.03 (t, 2H), 1.83 (m, 2H), 1.49 (m, 2H), 1.37 (m, 16H), 0.92 (t, 3H); ^{13}C NMR (400 MHz, $CDCl_3$); IR (ν/cm^{-1}): 2916, 2847; Elemental Analysis ($C_{24}H_{33}IO$: 464.42) Calcd: C, 62.07; H, 7.16. Found: C, 61.92; H, 7.08.

2.3. Gelation Study. According to previous procedures,[39] the synthesized organogelators **3a**−**c** were dissolved in various solvents and boiled in a sealed glass tube to produce a colorless medium and then cooled back to room temperature to generate the corresponding organogels. The organogels were formed in 15−25 min. The gelation time usually depends on the gelator's total content and the aliphatic tail length. The gelation process was verified by the "stable-to-inversion" technique as designated by the solvent disappearance. The reversibility was inspected by increasing the temperature (2 °C/min) of the organogel-containing tube and recording the gel melting point at which the organogel falls down. The above procedure was carried out several times to indicate good reversibility.

2.4. Apparatus and Methods. *2.4.1. Spectroscopic Characterization.* The melting points were recorded by differential scanning calorimetry (TA2920). Bruker Avance 400 MHz was used to collect the ^{1}H/^{13}C NMR spectra. For the elemental analysis, PerkinElmer 2400 (United States) was employed. UV−vis absorption spectra were measured using an Ultraviolet Agilent system from the Cary Series. Varian Cary Eclipse was utilized to study fluorescence and quantum yields (QY). To measure fluorescence QY, both rhodamine 101 (QY = 0.96) and rhodamine 6G (QY = 0.95) were used in ethyl alcohol (100%) as standards. The infrared spectra were obtained by Fourier transform infrared (FT-IR) using Bruker Vectra 33.

2.4.2. Morphological Characterization. The morphology of **3a** (partial gel) was studied by JEOL 1230 TEM (Japan). The partial organogel of **3a** in *n*-octanol was diluted and dropped onto a copper grid for TEM analysis. The SEM studies of **3b** and **3c** were carried out using the Quanta FEG 250 instrument (Republic of Czech). *n*-Octanol was used to prepare organogels from the corresponding gelators, which were subsequently air-dried on a piece of glass. The Au-coated dried gel was annealed at 45 °C overnight. The diameters of the produced supramolecular structures were measured using the ImageJ program (SEM).

2.5. Cytotoxic (In Vitro) and Antimicrobial Studies. The skin fibroblast cell line (BJ1) was utilized to carry out the cytotoxic study according to the MTT proliferation proce-

https://doi.org/10.1021/acsomega.2c03838
ACS Omega 2022, 7, 34309−34316

dure.[40] The antibacterial activity of the synthesized diphenyl ethers was investigated against *E. coli* (ATCC 25922) and *S. aureus* (ATCC 29213) using the AATCC 100:(1999) standard procedure.[41]

3. RESULTS AND DISCUSSION

3.1. Synthesis and Chemistry. The main aim of the current study is to synthesize novel fluorescent diphenyl ether gelators substituted with para-alkoxy groups of different aliphatic chain lengths. The synthesis was performed by reacting hydroxyl-substituted diphenyl with various alcohols of different aliphatic chain lengths. As shown in Scheme 1, the

Scheme 1. Synthesis of Alkoxy-Substituted Diphenyl Ether Organogelators 3a−c; *R* = C_3H_7; C_6H_{13}; $C_{11}H_{23}$

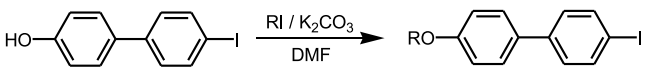

alkoxy-substituted diphenyl ethers (**3a**, **3b**, and **3c**) were prepared in comparatively high yields by treating a mixture of 4-alkoxy-4′-iodobiphenyl and *n*-iodoalkane with K_2CO_3 in DMF at room temperature. $^1H/^{13}C$ NMR and infrared analyses were utilized to verify the chemical structure of the synthesized diphenyl ethers **3a−c**. The ^1H NMR spectral analysis of **3a−c** showed distinctive peaks for the alkyl groups ranging from ∼0.92 to ∼4.03 ppm. The FT-IR spectral analysis of **3a−c** displayed strong absorption bands of alkyl substituents at ∼2950 and ∼2860 cm^{-1}.

3.2. Photophysical Studies. A light-responsive compound is able to transform its physical and/or chemical properties in response to a light stimulus.[42−44] In the current study, some selected solvents were utilized to inspect both absorption and emission behaviors of the prepared diphenyl ethers, as demonstrated in Table 1. Both emission and absorption maxima were determined in a range of solvents like dimethyl sulfoxide (DMSO), acetonitrile, hexane, *n*-octanol, tetrahydrofuran (THF), absolute ethanol, DMF, toluene, benzene, CH_2Cl_2, and *n*-propanol. Figure 1 displays the solution of **3b** in DMSO under visible and ultraviolet lights. It was observed that all diphenyl ethers absorb light in the

Table 1. Absorbance (abs) and Emission (em) Maxima in a Range of Solvents

	λ_{max} (nm)					
	3a		**3b**		**3c**	
solvents	abs	em	abs	em	abs	Em
ethanol	351	395	353	385	368	379
hexane	347	399	359	388	363	378
n-propanol	345	397	349	385	366	375
DMF	351	388	357	386	359	381
CH_2Cl_2	352	398	356	389	361	371
$CHCl_3$	354	391	358	390	365	379
n-octanol	343	396	353	386	369	385
toluene	345	389	350	386	367	378
1,2-dichloroethane	342	389	359	384	366	381
acetonitrile	347	385	352	375	358	369
THF	346	384	351	373	357	374
DMSO	344	386	348	377	366	370
benzene	350	391	356	383	351	378
ethylacetate	345	383	349	372	365	367

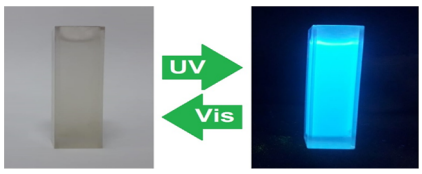

Figure 1. Solution of **3b** in DMSO under visible and ultraviolet lights.

ultraviolet−visible spectrum range. It can be concluded that the $\pi-\pi^*$ transition is the main reason for these absorption peaks.[45] The absorption maxima were observed to increase when extending the aliphatic tail length, indicating that the excitation state of the shorter aliphatic tail-bearing diphenyl ether is less than that of the longer aliphatic chain-bearing diphenyl ether. When the aliphatic tail length was increased, the absorption wavelength was found to increase in association with a decrease in the emission wavelength. Solvatochromic behavior was detected in the absorption and emission spectra as a function of solvent polarity. Both absorption and fluorescence wavelengths were found to increase when increasing the solvent polarity, indicating positive solvatochromism. Moreover, the quantum yields were observed to decrease when the aliphatic tail length increased.

3.3. Gelation Studies. The self-assembled nanofeather-like structures of the alkoxy-substituted π-conjugated diphenyl ethers have been reported. Light emission of a material has been a key character when being responsive to the surrounding environment. For instance, the generation of fluorescent supramolecular architectures could result in considerable modulated impact on the emission intensity and/or wavelength. Hence, assembled structures with fluorescence properties are priceless materials for the detection of diverse analytes. The propyloxy-substituted diphenyl ether **3a** demonstrated no gelation in various solvents. On the other hand, the hexyloxy- and undecyloxy-substituted diphenyl ethers **3b** and **3c** demonstrated good gelation properties in various solvents. The synthesized alkoxy-substituted diphenyl ether gelators consist of terminal aliphatic flexible tails and a rigid diphenyl core accountable for π-stacks. The aggregations of those diphenyl ether molecular gelators provide three-dimensional highly ordered nanofeather-like entanglements, which can be tuned by the ability to generate crystals and the extent of solubility. The synthesized organogelators (**3a−c**) are soluble when heated in a number of solvents. At room temperature, a soft gel was produced and observed by the "stable-to-inversion" technique as demonstrated in Figure 2. The creation of organogels from compounds **3a−c** was investigated in various solvents. The CGC can be defined as the minimum gelator concentration able to generate a stable organogel after thermal treatment according to the "stable-to-inversion" technique.[39] Different samples were prepared by decreasing the gelator concentration in the same solvent. Then, the "stable-to-inversion" procedure is applied to generate a stable organogel. Thus, the lowest gelator concentration with the ability to produce a stable organogel in the same solvent is defined as the critical gelation concentration. The CGC of hexyloxy-substituted diphenyl ether organogels was observed to be solvent-dependent in the range of 1.61−8.14 mM. The organogelator **3b** showed a substantial ability to gelate various solvents like ethylacetate, *n*-propanol, DMSO, and *n*-octanol. Nonetheless, compound **3b** was found to incompletely gelate other solvents like acetonitrile and toluene. Compound **3b**

https://doi.org/10.1021/acsomega.2c03838
ACS Omega 2022, 7, 34309−34316

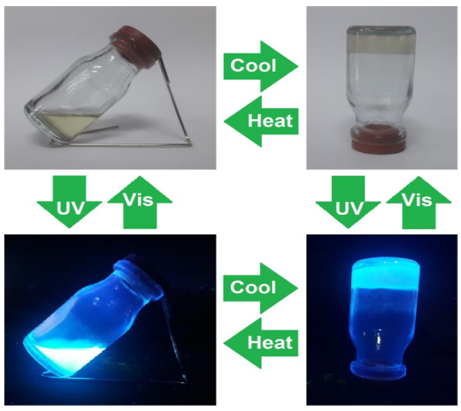

Figure 2. Thermal and fluorescence reversibilities of organogel (**3b**) in DMSO under visible and ultraviolet lights.

showed no gelation in ethanol, DMF, THF, 1,2-dichloroethane, CH_2Cl_2, $CHCl_3$, hexane, or benzene. The gelation properties of the diphenyl ether gelators **3a–c** in a variety of solvents are summarized in Table 2. The propyloxy-substituted diphenyl ether **3a** displayed low solubility. Therefore, it precipitates in various solvents. The undecyloxy-substituted diphenyl ether **3c** displayed a very high solubility. Thus, it forms clear solutions in many solvents at room temperature. The formed organogels were either colorless or white soft materials. The thermal reversibility between sol and gel was highly accomplished. The generated gels showed photophysical properties almost identical to those observed for their corresponding solution states. The aliphatic tails are nonpolar groups with a single bond between carbon and hydrogen atoms. Hence, the attraction forces between those aliphatic tails are relatively weak London dispersion (van der Waals) attraction forces, which typically strengthen with increasing the aliphatic tail length due to increasing the molecular surface area. Therefore, the hexyloxy- and undecyloxy-substituted diphenyl ethers with longer alkyl tails (**3b** and **3c**) have shown enhanced gelation properties as compared to the propyloxy-substituted diphenyl ether **3a,** comprising a shorter alkyl tail.

Table 2. Gelation Screening of Alkoxy-Substituted Diphenyl Ethers 3a–c in a Variety of Solvents; G = Gel; PG = Partial Gel; Sol = Solution; P = Precipitate; CGC (mM)

	gelation screening		
solvent	**3a**	**3b**	**3c**
ethylacetate	PG	G (2.42 mM)	PG
THF	Ppt	sol	sol
DMF	sol	sol	sol
CH_2Cl_2	sol	sol	sol
$CHCl_3$	sol	sol	sol
n-propanol	PG	G (8.14 mM)	PG
n-octanol	PG	G (1.61 mM)	G (4.36 mM)
1,2-dichloroethane	Ppt	ppt	sol
acetonitrile	PG	PG	PG
hexane	Ppt	Ppt	Ppt
DMSO	sol	G (2.76 mM)	G (3.71 mM)
ethanol	Ppt	Ppt	sol
toluene	PG	PG	PG
benzene	Ppt	Ppt	Ppt

As demonstrated in Figure 3, a blue shift was detected in the fluorescence maximum wavelength for the gel state of **3b** as compared to the fluorescence maximum wavelength for a diluted solution of **3b** (sol state) in DMSO. This could be attributed to the formation of H-aggregates' organogel.[46] H-aggregations have a tendency to produce 2D nanofeather-like architectures owing to the intermolecular van der Waals attraction forces of the terminal alkoxy groups in collaboration with intermolecular π-stacks of the diphenyl core.

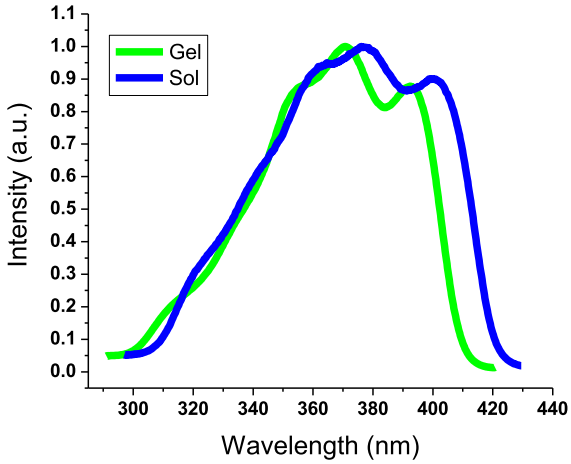

Figure 3. Normalized fluorescence of **3b** in both the gel and sol (DMSO; 2.14×10^{-5} mol/L) phases.

Table 3 summarizes quantum yields of **3a–c** in gel (or partial organogel) and solution states. The generated gels showed various fluorescence wavelengths in comparison to the sol state of a gelator. In DMSO, the sol state fluorescence of **3b** at 377 nm was found to shift to 371 nm for the gel phase. The incomplete gelation showed lower shift activity in the emission wavelengths as compared to the complete gelation cases. The quantum yields of **3a** and **3b** increased in the gel state in comparison to the solution state.[39]

The thermal stability of the diphenyl ether organogel **3b** in octyl alcohol was studied by reporting the CGC-dependent gel → sol transition as shown in Figure 4. The gel melting point was found to increase from 38 to 49 °C when increasing the gelator concentration from 1.6 to 15.0 mmol L^{-1}, respectively. The enhanced thermal stability could be attributed to the high gelator density in the nanofeather matrix. Nonetheless, the gel melting point decreased when increasing the gelator total content above 15.0 mmol/L.

The temperature-dependent transition was studied to examine the gel–sol reversibility (Figure 5). The soft gel was heated to 195 °C until it formed a colorless solution. During the heating process, the gel's collapsing temperature was recorded. The solution-containing glass vial was then left to settle for a few minutes at 25 °C, allowing the gel to regenerate as demonstrated by the "stable-to-inversion" technique. The exceeding procedures were repeated in several cycles to verify no changes in the gel → sol transition temperature, confirming excellent reversibility.

3.4. Morphologies and Assemblies. Utilizing both SEM and TEM analyses, the morphologies of the diphenyl ether xerogels **3a–c** were studied. Depending on the length of the aliphatic chain, various supramolecular morphologies were monitored, including nanofeathers, nanofibers, and nanosheets. The self-assembled nanofeathers of **3b** were observed to be

https://doi.org/10.1021/acsomega.2c03838
ACS Omega 2022, 7, 34309–34316

Table 3. Fluorescence QY of 3a−c in Gel (Partial Gelation) and Sol (2.14×10^{-5} mol/L) Phases; λ_{em} (nm) Is the Emission Maximum Wavelength

	3a				3b				3c			
	solution		gel		solution		gel		solution		gel	
solvent	λ_{em}	QY	λ_{em}	QY	λ_{em}	QY	λ_{em}	QY	λ_{em}	QY	λ_{em}	QY
n-propanol	397	0.52	388	0.56	385	0.67	375	0.54	375	0.27	367	0.30
n-octanol	396	0.34	384	0.44	386	0.30	371	0.36	385	0.31	364	0.36
ethylacetate	383	0.43	371	0.45	372	0.32	360	0.44	367	0.26	355	0.35
DMSO	386	0.32	375	0.48	377	0.43	371	0.54	370	0.21	358	0.40
acetonitrile	385	0.25	376	0.34	375	0.31	362	0.45	369	0.23	353	0.27
toluene	389	0.34	373	0.33	386	0.28	379	0.33	378	0.26	357	0.31

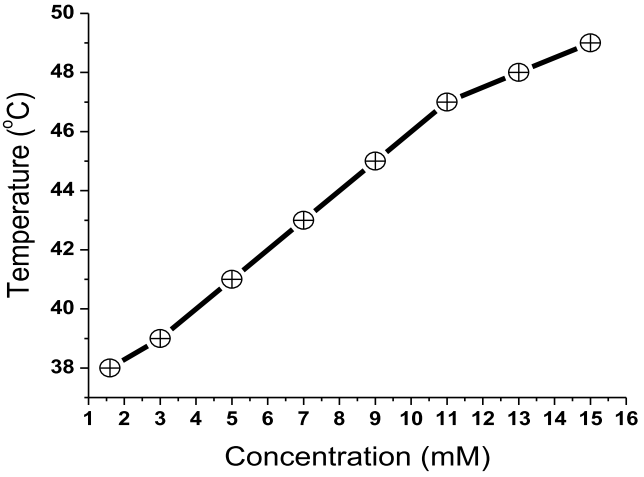

Figure 4. Gel → sol transition of **3b** vs its concentration in *n*-octanol.

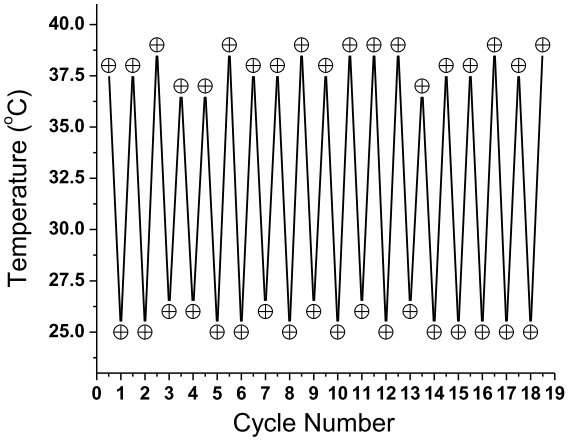

Figure 5. Reversibility of the diphenyl ether **3b**.

strongly ordered and consistent. SEM micrographs were utilized to inspect the morphological aggregations of **3b** and **3c** xerogels, as shown in Figures 6 and 7. The gel was dropped onto a piece of glass and left to air-dry overnight to provide xerogel. SEM images demonstrated the formation of three-dimensional self-assembled architectures due to the immobilization of solvent molecules. SEM micrographs showed highly ordered nanofeather-like supramolecular porous assemblies to indicate strong intermolecular attraction forces. Self-assembly into nanofeathers with a width in the range of 220−410 nm and a length of few microns was observed in SEM images of **3b** due to immobilization of *n*-octanol molecules (Figure 6). On the other hand, multilayer-like supramolecular architectures

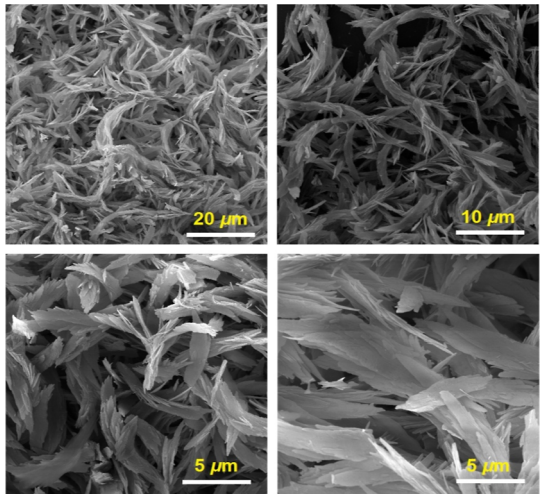

Figure 6. SEM graphs of **3b** xerogel demonstrating nanofeather-like supramolecular morphologies due to immobilization of *n*-octanol.

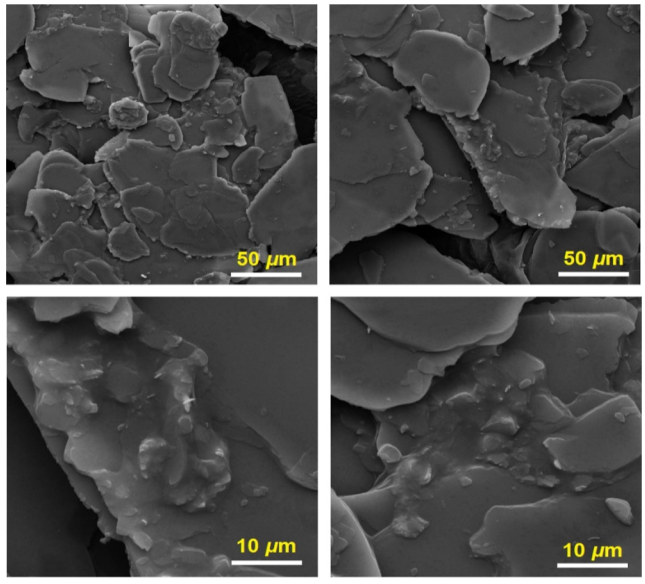

Figure 7. SEM graphs of **3c** xerogel demonstrating nanosheet-like supramolecular morphologies due to immobilization of *n*-octanol molecules.

(nanosheets) were observed in the SEM images of **3c** upon immobilizing the *n*-octanol molecules (Figure 7). The morphology of **3a** (partial gel) was determined after dilution in *n*-octanol, as shown in Figure 8. One-dimensional nanofibrous supramolecular architectures were detected for

https://doi.org/10.1021/acsomega.2c03838
ACS Omega 2022, 7, 34309−34316

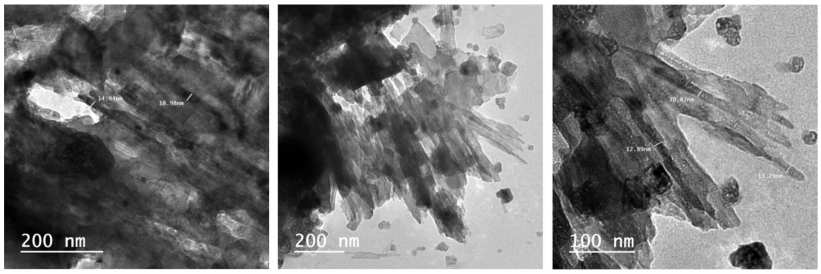

Figure 8. TEM graphs of **3a** (partial gel) diluted by *n*-octanol demonstrating nanofibrous-like supramolecular morphologies.

the partial organogel generated by **3a**. TEM images of **3a** (partial gel) showed nanofibers with diameters of 10−19 nm and a length of few microns. Upon increasing the aliphatic tail length, the highly ordered supramolecular porous self-assembly monitored for **3b** decreases to less ordered and less porous supramolecular architectures as monitored for **3c**. This could be attributed to decreasing the intermolecular attraction forces when increasing the aliphatic tail length. Thus, the length of the alkoxy tail was monitored as a key element in enhancing the gelator stability.

3.5. Biological Properties. The synthesized gelators **3a−c** were examined for their cytotoxicity to report the viability of BJ1 cells upon exposure to those alkoxy-substituted diphenyl ethers. Both **3a** and **3b** displayed no effect on cell proliferation. On the other hand, gelator **3c** starts to mislay its viability, resulting in viable cells of 92.57%. Due to the precipitation tendency of organic compounds from solutions, there is less space for the growth of cells, leading to a decrease in cell numbers. Therefore, the alkoxy-substituted diphenyl ethers **3a** and **3b** are evidently harmless. Hence, those compounds can be possibly utilized for drug delivery purposes. Additionally, the antimicrobial activity was tested against *E. coli* and *S. aureus*, demonstrating satisfactory antibacterial performance, as summarized in Table 4. Nonetheless, the antibacterial performance decreased on extending the aliphatic tail length.

Table 4. Antimicrobial Properties of Diphenyl Ethers

	reduction %	
compound	*S. aureus*	*E. coli*
3a	17 ± 1.1	18 ± 1.1
3b	19 ± 1.0	22 ± 1.0
3c	26 ± 1.2	28 ± 1.4

4. CONCLUSIONS

A series of alkoxy-substituted iodo-biphenyl ethers able to self-assemble into nanofeather-like supramolecular architectures were synthesized and studied by various spectroscopic methods. The presence of the iodo-biphenyl moiety and alkoxy groups was monitored to gelate organic solvents into highly ordered self-assembled nanofeather-like supramolecular architectures. The suitable molecular combination of the iodo-biphenyl moiety with the terminal aliphatic tails facilitated the creation of those supramolecular architectures. The characteristic self-assembly of those alkoxy-substituted iodo-biphenyl ethers into nanostructural assemblies was inspected by SEM and TEM analysis techniques. Depending on the aliphatic chain length, different morphologies were observed, including nanofeathers, nanosheets, and nanofibers. SEM micrographs of the undecyloxy-substituted diphenyl ether xerogel showed highly ordered nanofeather-like supramolecular porous assemblies (220−410 nm) to indicate strong intermolecular attraction forces. On the other hand, multilayer-like architectures (nanosheets) were observed for the hexyloxy-substituted diphenyl ether xerogel. The morphology of the propyloxy-substituted diphenyl ether partial gel displayed one-dimensional nanofibrous supramolecular assemblies of nanofibers with diameters of 10−19 nm. The creation of nanofeathers could be ascribed to π-stacking of the iodo-biphenyl moiety in collaboration with van der Waals attraction forces of long aliphatic tails. The present alkoxy-substituted iodo-biphenyl gelators were observed to be non-cytotoxic with satisfactory antibacterial properties...

■ ASSOCIATED CONTENT

Supporting Information

The Supporting Information is available free of charge at https://pubs.acs.org/doi/10.1021/acsomega.2c03838.

Thermal and fluorescence reversibility of organogels under visible and ultraviolet lights and ^{1}H NMR spectra of the compounds prepared in the study (PDF)

■ AUTHOR INFORMATION

Corresponding Author

Nashwa M. El-Metwaly − *Department of Chemistry, Faculty of Applied Science, Umm Al-Qura University, Makkah 24230, Saudi Arabia; Department of Chemistry, Faculty of Science, Mansoura University, Mansoura 35516, Egypt;* orcid.org/0000-0002-0619-6206; Email: n_elmetwaly00@yahoo.com, nmmohamed@uqu.edu.sa

Authors

Matokah M. Abualnaja − *Department of Chemistry, Faculty of Applied Science, Umm Al-Qura University, Makkah 24230, Saudi Arabia*

Abdulmajeed F. Alrefaei − *Department of Biology/Genetic and Molecular Biology Central Laboratory (GMCL), Jamoum University College, Umm Al Qura University, Makkah 2203, Saudi Arabia*

Hana M. Abumelha − *Department of Chemistry, College of Science, Princess Nourah Bint Abdulrahman University, Riyadh 11671, Saudi Arabia*

Omaymah Alaysuy − *Department of Chemistry, College of Science, University of Tabuk, Tabuk 71474, Saudi Arabia*

Amal T. Mogharbel − *Department of Chemistry, College of Science, University of Tabuk, Tabuk 71474, Saudi Arabia*

Albandary Almahri − *Department of Chemistry, College of Science and Humanities in Al-Kharj, Prince Sattam Bin Abdulaziz University, Al-Kharj 11942, Saudi Arabia*

https://doi.org/10.1021/acsomega.2c03838
ACS Omega 2022, 7, 34309−34316

Complete contact information is available at:
https://pubs.acs.org/10.1021/acsomega.2c03838

Notes

The authors declare no competing financial interest.
All relevant data are within the manuscript and available from the corresponding author upon request.

■ ACKNOWLEDGMENTS

Princess Nourah bint Abdulrahman University Researchers Supporting project number (PNURSP2022R22), Princess Nourah bint Abdulrahman University, Riyadh, Saudi Arabia.

■ REFERENCES

(1) Kamitani, T.; Ishida, A.; Imoto, H.; Naka, K. Supramolecular organogel of polyureas containing POSS units in the main chain: dependence on the POSS and comonomer structures. *Polym. J.* **2022**, *54*, 161−167.
(2) Pang, S.; Chen, H.; Jiang, Z.; Song, B.; Xie, D.; Zhai, Z.; Cui, Z.; Gu, Y.; Pei, X. Water-in-Oil Emulsion Gels Stabilized by a Low-Molecular Weight Organogelator Derived from Dehydroabietic Acid. *Langmuir* **2022**, *38*, 6049−6056.
(3) Saha, E.; Karthick, K.; Kundu, S.; Mitra, J. Electrocatalytic Oxygen Evolution in Acidic and Alkaline Media by a Multistimuli-Responsive Cobalt(II) Organogel. *ACS Sustain. Chem. Eng.* **2019**, *7*, 16094−16102.
(4) Khattab, T. A.; El-Naggar, M. E.; Abdelrahman, M. S.; Aldalbahi, A.; Hatshan, M. R. Simple Development of Novel Reversible Colorimetric Thermometer Using Urea Organogel Embedded with Thermochromic Hydrazone Chromophore. *Chemosensors* **2020**, *8*, 132.
(5) Altoom, N. G. Synthesis and characterization of novel fluoroterphenyls: self-assembly of low-molecular-weight fluorescent organogel. *Luminescence* **2021**, *36*, 1285−1299.
(6) Cherumukkil, S.; Das, G.; Tripathi, R. P. N.; PavanKumar, G. V.; Varughese, S.; Ajayaghosh, A. π-Extended Bodipy Self-Assembly as Supramolecular Photonic Security Ink and Optical Waveguide. *Adv. Funct. Mater.* **2022**, *32*, 2109041.
(7) Khattab, T. A. Synthesis and Self-assembly of Novel s-Tetrazine-based Gelator. *Helv. Chim. Acta* **2018**, *101*, No. e1800009.
(8) Babu, S. S.; Praveen, V. K.; Ajayaghosh, A. Functional π-gelators and their applications. *Chem. Rev.* **2014**, *114*, 1973−2129.
(9) Abualnaja, M. M.; Hossan, A.; Bayazeed, A.; Al-Qahtani, S. D.; Al-Ahmed, Z. A.; Abdel-Hafez, S. H.; El-Metwaly, N. M. Synthesis and self-assembly of new fluorescent cholesteryloxy-substituted fluorinated terphenyls with gel formation and mesogenic phases. *J. Mol. Struct.* **2022**, *1251*, 132006.
(10) Kartha, K. K.; Dev Mukhopadhyay, R.; Ajayaghosh, A. Supramolecular gels and functional materials research in India. *Chimia* **2013**, *67*, 51.
(11) Khattab, T. A.; El-Naggar, M. E.; Al-Sehemi, A. G.; Al-Ghamdi, A. A.; Taleb, M. F. Novel fluorescent nanofibrous polyether template developed by SNAr polymerization of fluoroaryl-containing 1, 3, 4-oxadiazole: Photophysical properties, mesogenic phases and self-assembly. *Eur. Polym. J.* **2022**, *173*, 111270.
(12) Das, G.; Thirumalai, R.; Vedhanarayanan, B.; Praveen, V. K.; Ajayaghosh, A. Enhanced Emission in Self-Assembled Phenyleneethynylene Derived π-Gelators. *Adv. Opt. Mater.* **2020**, *8*, 2000173.
(13) Kartha, K. K.; Sandeep, A.; Praveen, V. K.; Ajayaghosh, A. Detection of nitroaromatic explosives with fluorescent molecular assemblies and π-gels. *Chem. Rec.* **2015**, *15*, 252−265.
(14) Kim, D.; Kwon, J. E.; Park, S. Y. Fully reversible multistate fluorescence switching: organogel system consisting of luminescent cyanostilbene and turn-on diarylethene. *Adv. Funct. Mater.* **2018**, *28*, 1706213.
(15) Zhang, T.; Chen, F.; Zhang, C.; Che, X.; Li, W.; Bai, B.; Wang, H.; Li, M. Multistimuli-responsive fluorescent organogelator based on triphenylamine-substituted acylhydrazone derivative. *ACS Omega* **2020**, *5*, 5675−5683.
(16) Kartha, K. K.; Babu, S. S.; Srinivasan, S.; Ajayaghosh, A. Attogram sensing of trinitrotoluene with a self-assembled molecular gelator. *J. Am. Chem. Soc.* **2012**, *134*, 4834−4841.
(17) Moharana, P.; Santosh, V. Organogels Fabricated from Self-Assembled Nanotubes Containing Core Substituted Perylene Diimide Derivative. *ACS Omega* **2022**, *7*, 21932−21938.
(18) Bonifazi, E. L.; Mac Cormack, A. S.; Busch, V. M.; Japas, M. L.; Di Bari, L.; Di Chenna, P. H. Chiral self-assembly and water effect on a supramolecular organogel stable towards aqueous interfaces. *J. Solgel Sci. Technol.* **2022**, *102*, 30−40.
(19) Zhu, J.; Zhang, T.; Liu, Y.; Lu, D.; Zhang, P.; Li, M.; Wang, H.; Wen, M. Fabrication of a superhydrophobic surface by modulating the morphology of organogels. *Soft Matter* **2021**, *17*, 3745−3752.
(20) Giuri, D.; Zanna, N.; Tomasini, C. Low molecular weight gelators based on functionalized l-dopa promote organogels formation. *Gels* **2019**, *5*, 27.
(21) Ni, Y.; Li, X.; Hu, J.; Huang, S.; Yu, H. Supramolecular liquid-crystalline polymer organogel: Fabrication, multiresponsiveness, and holographic switching properties. *Chem. Mater.* **2019**, *31*, 3388−3394.
(22) Aykent, G.; Zeytun, C.; Marion, A.; Özçubukçu, S. Simple tyrosine derivatives act as low molecular weight organogelators. *Sci. Rep.* **2019**, *9*, 4893.
(23) Ishida, A.; Fujii, S.; Sumida, A.; Kamitani, T.; Minami, S.; Urayama, K.; Imoto, H.; Naka, K. Supramolecular organogel formation behaviors of beads-on-string shaped poly (azomethine) s dependent on POSS structures in the main chains. *Polym. Chem.* **2021**, *12*, 3169−3176.
(24) Chen, X.; Zhou, Y.; Yang, M.; Wang, J.; Guo, C.; Wang, Y. A novel multi-stimuli-responsive organogel sensor for detecting Cu2+ and Co2+ based on benzotriazole derivative. *J. Mol. Struct.* **2022**, *1250*, 131810.
(25) Mosquera Narvaez, L. E.; Ferreira, L. M.; Sanches, S.; Alesa Gyles, D. A.; Silva-Júnior, J. O. C.; Ribeiro Costa, R. M. A Review of Potential Use of Amazonian Oils in the Synthesis of Organogels for Cosmetic Application. *Molecules* **2022**, *27*, 2733.
(26) Loos, J. N.; D'Acierno, F.; Vijay Mody, U. V.; MacLachlan, M. J. Manipulating the Self-Assembly of Multicomponent Low Molecular Weight Gelators (LMWGs) through Molecular Design. *ChemPlusChem* **2022**, *87*, No. e202200026.
(27) Luo, M.; Wang, S.; Li, C.; Miao, W.; Ma, X. Aggregation-induced emission organogel formed by both sonication and thermal processing based on tetraphenylethylene and cholesterol derivative. *Dyes Pigm.* **2019**, *165*, 436−443.
(28) Safiullina, A. S.; Ziganshina, S. A.; Lyadov, N. M.; Klimovitskii, A. E.; Ziganshin, M. A.; Gorbatchuk, V. V. Role of water in the formation of unusual organogels with cyclo (leucyl−leucyl). *Soft Matter* **2019**, *15*, 3595−3606.
(29) Ji, W.; Yuan, C.; Wang, F.; Liu, J.; Qin, M.; Yan, X.; Feng, C. Deciphering the structure-property relationship in coumarin-based supramolecular organogel materials. *Colloids Surf. A Physicochem. Eng. Asp.* **2020**, *597*, 124744.
(30) Mandegani, F.; Zali-Boeini, H.; Khayat, Z.; Scopelliti, R. A smart low molecular weight gelator for the triple detection of copper(II), mercury(II), and cyanide ions in water resources. *Talanta* **2020**, *219*, 121237.
(31) Chetia, M.; Debnath, S.; Chowdhury, S.; Chatterjee, S. Self-assembly and multifunctionality of peptide organogels: Oil spill recovery, dye absorption and synthesis of conducting biomaterials. *RSC Adv.* **2020**, *10*, 5220−5233.
(32) Huang, Y.; Liu, S.; Xie, Z.; Sun, Z.; Chai, W.; Jiang, W. Novel 1,2,3-triazole-based compounds: Iodo effect on their gelation behavior and cation response. *Front. Chem. Sci. Eng.* **2018**, *12*, 252−261.
(33) Huang, Y.; Zhang, Y.; Yuan, Y.; Cao, W. Organogelators based on iodo 1,2,3-triazole functionalized with coumarin: properties and gelator-solvent interaction. *Tetrahedron* **2015**, *71*, 2124−2133.

(34) Khattab, T. A.; Tiu, B. D. B.; Adas, S.; Bunge, S. D.; Advincula, R. C. pH triggered smart organogel from DCDHF-Hydrazone molecular switch. *Dyes Pigm.* **2016**, *130*, 327−336.
(35) Hossan, A.; Abumelha, H. M.; Alnoman, R. B.; Bayazeed, A.; Alsoliemy, A.; Keshk, A. A.; El-Metwaly, N. M. Synthesis, self-assembly and optical properties of novel fluorescent alkoxy-substituted fluoroaryl 1, 3, 4-oxadiazole organogelator. *Arabian J. Chem.* **2022**, *15*, 103771.
(36) Abdelrahman, M. S.; Khattab, T. A.; Kamel, S. Hydrazone-Based Supramolecular Organogel for Selective Chromogenic Detection of Organophosphorus Nerve Agent Mimic. *ChemistrySelect* **2021**, *6*, 2002−2009.
(37) Alsoliemy, A.; Alrefaei, A. F.; Almehmadi, S. J.; Almehmadi, S. J.; Hossan, A.; Khalifa, M. E.; El-Metwaly, N. M. Synthesis, characterization and self-assembly of new cholesteryl-substitued sym-tetrazine: Fluorescence, gelation and mesogenic properties. *J. Mol. Liq.* **2021**, *342*, 117543.
(38) Radwan, A. S.; Makhlouf, M. M. Synthesis, characterization, and self-assembly of fluorescent fluorine-containing liquid crystals. *Luminescence* **2021**, *36*, 1751−1760.
(39) Al-Qahtani, S. D.; Snari, R. M.; Bayazeed, A.; Alnoman, R. B.; Hossan, A.; Alsoliemy, A.; El-Metwaly, N. M. Synthesis, characterization and self-assembly of novel fluorescent alkoxy-substituted 1, 4-diarylated 1, 2, 3-triazoles organogelators. *Arabian J. Chem.* **2022**, *15*, 103874.
(40) Khattab, T. A.; Tolba, E.; Gaffer, H.; Kamel, S. Development of electrospun nanofibrous-walled tubes for potential production of photoluminescent endoscopes. *Ind. Eng. Chem. Res.* **2021**, *60*, 10044−10055.
(41) Singh, P. K.; Goyal, M. Green Synthesis Using Klebsiella pneumoniae as well as its Execution onto Textiles for Microbe Resistance. *IOP Conf. Ser.: Mater. Sci. Eng.* **2020**, *988*, 012071.
(42) Panja, S.; Adams, D. J. Stimuli responsive dynamic transformations in supramolecular gels. *Chem. Soc. Rev.* **2021**, *50*, 5165−5200.
(43) Yu, L.; Zhao, R.; Wang, N.; Feng, S.; Xu, X.-D. X.-D. Coordination Mode-Regulated Lanthanide Supramolecular Hydrogels with Tunable Luminescence and Stimuli-Responsive Properties. *ACS Appl. Polym. Mater.* **2021**, *3*, 3623−3630.
(44) Wang, Y.; Chen, J.; Shang, Y.; Li, P.; Li, H. A stimuli responsive lanthanide-based hydrogel possessing tunable luminescence by efficient energy transfer pathways. *J. Rare Earths* **2022**, *40*, 696−701.
(45) Cai, W.; Xu, D.; Qian, L.; Wei, J.; Xiao, C.; Qian, L.; Lu, Z.-Y.; Cui, S. Force-Induced Transition of π-π Stacking in a Single Polystyrene Chain. *J. Am. Chem. Soc.* **2019**, *141*, 9500−9503.
(46) Alqarni, S. A.; Al-Qahtani, S. D.; Alluhaybi, A. A.; Alnoman, R. B.; Alsoliemy, A.; Abdel-Hafez, S. H.; El-Metwaly, N. M. Development of a Fluorescent Nanofibrous Template by In Situ SNAr Polymerization of Fluorine-Containing Terphenyls with Aliphatic Diols: Self-Assembly and Optical and Liquid Crystal Properties. *ACS Omega* **2021**, *6*, 35030−35038.

https://doi.org/10.1021/acsomega.2c03838
ACS Omega 2022, 7, 34309−34316